Relationship between Crystalline Orientations of Gold and Surface-Enhanced Raman Scattering Spectroscopy of Polypyrrole and Mechanism of Roughening Procedure on Gold via Cyclic Voltammetry

Yu-Chuan Liu* and Li-Yuan Jang

Department of Chemical Engineering, Van Nung Institute of Technology, 1, Van Nung Road, Shuei-Wei Li, Chung-Li City, Taiwan, Republic of China

Received: March 6, 2002

The polypyrrole (PPy) films were electrochemically deposited on roughened gold substrates with different predominant crystalline orientations of (111) and (220), respectively. Gold was roughened via a cyclic voltammetry procedure. The result indicates that the (220) crystalline orientation of gold was partially changed into (111) one after gold was roughened with oxidation−reduction cycles (ORC) treatment. The surface-enhanced Raman scattering (SERS) spectroscopy of PPy deposited on gold with predominant (111) orientation exhibits higher intensity and more excellent resolution. Meanwhile, the redox behavior of gold and the resulting complex in ORC were strongly sensitive to the crystalline orientation. A mechanism of the roughening procedure on gold was also proposed to illustrate the resulting complex and its effect on the SERS enhancement.

Introduction

Raman spectroscopy is an essential method to evaluate the structure situation of polypyrrole (PPy) in various states.[1,2] Nevertheless, only poor information can be provided due to weak signal or interference from noise.[3,4] On the whole, the Raman technique cannot be applied to the analysis of organic compounds that are present in a system at very low levels. However, resonance-enhanced Raman spectroscopy (RRS) and surface-enhanced Raman scattering (SERS) are two useful exceptions to this rule.[5,6] SERS occurring on roughened metal substrates in principle provides a powerful means of obtaining vibrational information on adsorbate−surface interactions in view of its unique sensitivity and excellent frequency resolution.[5] The mechanism of SERS as it is now generally accepted consists of two major components. One of the electromagnetic enhancement,[7,8] resulting from an apparent increase in the Raman cross section, is quite well understood. However, the other of the chemical enhancement,[9,10] concerning the charge transfer on the adsorbate−metal surface, is poorly understood compared to the electromagnetic enhancement. Generally, the electrochemical roughening of the surface can be carried out using two different procedures of oxidation−reduction cycles (ORC). One is a triangular-wave ORC,[11,12] the other is a square-wave ORC.[13,14] For producing a controllable surface roughness and a homogeneous surface, the former has an advantage over the latter.[15,16] In chemical enhancement, most studies[17−19] were devoted to molecules adsorbed on activated silver surfaces. A major limitation of silver is the relatively negative potentials at which anodic metal dissolution occurs.[11,13] Gold (Au) is a more suitable electrode from this point of view, since it provides an especially large polarizable potential window of about of 2 V even in aqueous media. Moreover, the corresponding SERS-active moieties on gold are of inherently greater stability than on silver.[20,21]

Parsons[22] reported that the behavior of polycrystalline metals is a complex average which is difficult to understand without measurement on simpler systems and the redox behavior of metal in cyclic voltammetry (CV) is markedly dependent on the face of crystal exposed. Also, Bukowska et al.[23] reported that the change of the surface structure via ORC treatment significantly influences the corresponding SERS effect. Furtak and Roy[24] reported that SERS is sensitive to molecular orientation and to direct proximity with the substrate. These studies revealed that the crystalline orientation of metal is an important factor influencing the SERS enhancement. Therefore, Sanda et al.[25] studied the vibrations and structure of pyridine chemisorbed on single-crystal Ag (111). Caldwell et al.[26] studied the highly ordered self-assembled monolayer film of an azobenzealkanethiol on single-crystal Au (111). Meanwhile, Gao et al.[21] reported that the intensity of pyridine adsorbed on silver roughened in 0.1 M KCl is higher than that adsorbed on roughened gold. On the contrary, the intensity of pyridine adsorbed on silver is lower than that adsorbed on gold in the case of the electrolyte used in roughening treatment being replaced by $NaClO_4$. Baibarac et al.[27] reported SERS spectra of emeraldine base films deposited on various roughened metals substrates. The results indicated two different aspects: the variation of the overall intensity of Raman radiation, and a change affecting the positions and especially the relative intensities of certain Raman spectrum lines. All of these results revealed that the some interactions must exist between adsorbates or deposited materials and roughened substrates.

Since SERS effect takes place at the interface of roughened metal, a complex film formed on the activated metal during an ORC treatment thus plays an important role. However, few efforts concerning the effects of metal orientations on the complex formed in ORC treatment and on the SERS effects had been made. In this study, PPy films were originally electropolymerized on Au substrates with different predominant orientations of (111) and (220), respectively, roughened by a

* Author to whom all correspondence should be addressed. Tel: 886-3-4515811#254. Fax: 886-2-86638557. E-mail: liuyc@cc.vit.edu.tw.

10.1021/jp020644o CCC: $22.00
Published on Web 06/12/2002

triangular-wave ORC in an aqueous solution to investigate the relationship between crystalline orientations of gold and SERS spectroscopy of PPy. Also a mechanism of the roughening procedure on gold was also proposed to illustrate the resulting complex and its effect on the SERS enhancement.

Experimental Section

PPy Films Deposited on Roughened Au Substrates. All the electrochemical experiments were performed in a three-compartment cell at room temperature, 24 °C, and were controlled by a potentiostat (model PGSTAT30, Eco Chemie). A sheet of gold foil with predominant crystalline orientation of (111) or (220) with a disk of 0.238 cm^2 working area, a 2 × 2 cm platinum sheet, and silver−silver chloride (Ag/AgCl) were employed as the working, counter, and reference electrodes, respectively. Before the electropolymerization of PPy the gold electrode was mechanically polished as smooth as a mirror then was roughened by ORC treatment in a separate cell. The electrode was cycled in a deoxygenated aqueous solution containing 0.1 M KCl from −0.28 V (holding 10 s) to 1.22 V (holding 5 s) at 500 mV/s for 25 times. Then the electrochemical synthesis of PPy on roughened gold was carried out at a constant anodic potential of 0.85 V in a deoxygenated aqueous solution containing 0.1 M pyrrole and 0.1 M $LiClO_4$. For different requirements, the charges used in depositing PPy were 500, 10, and 2 mC for X-ray diffraction, SERS, and X-ray photoelectron spectroscopy experiments, respectively.

Characteristics of PPy Deposited on Roughened Au. The structure orientations of gold substrates before and after roughening treatment and PPy films were determined via XRD (Model Dmax-B, Rigaku) analyses. Raman spectra were obtained using a Renishaw 2000 Raman spectrometer employing a He−Ne laser operating at 632.8 nm of 25 mW and a charge couple device (CCD) detector with 1 cm^{-1} resolution. For XPS measurements a Physical Electronics PHI 1600 spectrometer with monochromatized Mg Kα radiation, 15 kV 250 W, and an energy resolution of 0.1−0.8% $\Delta E/E$ was used. For avoiding interference from the bulk property of Au and corresponding with the experimental sensitivities, the redeposited gold powders after ORC treatment were carefully scraped down from the identical gold substrate and were collected several times in some XRD and XPS measurements.

Results and Discussion

Relationship between Crystalline Orientation of Gold and Its Redox Behavior in CV. Figure 1 shows typical cyclic voltammograms for the anodic dissolution and redeposition of silver and gold in aqueous 0.1 M KCl. The chloride electrolyte was selected since this facilitates the metal dissolution−deposition process that is known to yield SERS-active roughened surfaces.[28] Clearly, the roughened Ag electrode is unsuitable for depositing PPy on it at 0. 85 V vs Ag/AgCl used in this study because of its narrow polarizable potential window.

Prior to roughening, four gold substrates were performed XRD analyses, as shown in Figure 2. The peaks located at 38.2°, 44.4°, 64.6°, and 77.5° are assigned to (111), (200), (220), and (311) faces of Au. The predominant crystalline orientation of sample (a) is (220). In contrast, the (111) orientation is predominant for samples (b)−(d). For a qualitative expression, the ratio of the intensity of the (111) face to the intensity of the (220) face is calculated. These values are 0.245, 1.54, 6.54, and 9.41 for samples (a)−(d), respectively. Then these gold substrates were roughened by ORC treatment. Figure 3 shows the results of cyclic voltammograms for the dissolution and redeposition of Au substrates with different orientations. It is interesting that the redox behavior of gold in CV is strongly dependent on its crystalline orientation. Namely, the anodic peak at ca. 0.3 to 0.5 V vs Ag/AgCl shows significantly with an increase in the ratio of the intensity of the (111) face to the intensity of the (220) face of gold. However, this anodic peak disappears for sample (a) with predominant (220) orientation. Study by Gao et al.[21] showed the result similar to that of sample (a) in Figure 3, and it results chiefly in the formation of $AuCl_4^-$. Nevertheless, the appearance of the anodic peak in CV for Au with predominant (111) face is scarcely reported in the literature. Furthermore, the colors of redeposited gold powders on the gold substrates with predominant (111) and (220) faces are bright and pale tan, respectively. Also, the decrease in mass of gold with a predominant (111) face after ORC is less. All these qualitative differences reveal that the complexes formed during ORC on gold with different crystalline orientation are distinct.

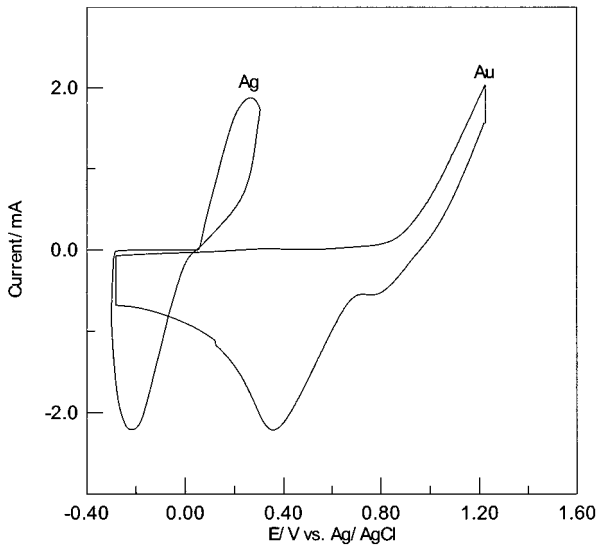

Figure 1. Cyclic voltammograms at 500 mV/s of the third scan for silver and gold electrodes in 0.1 M KCl.

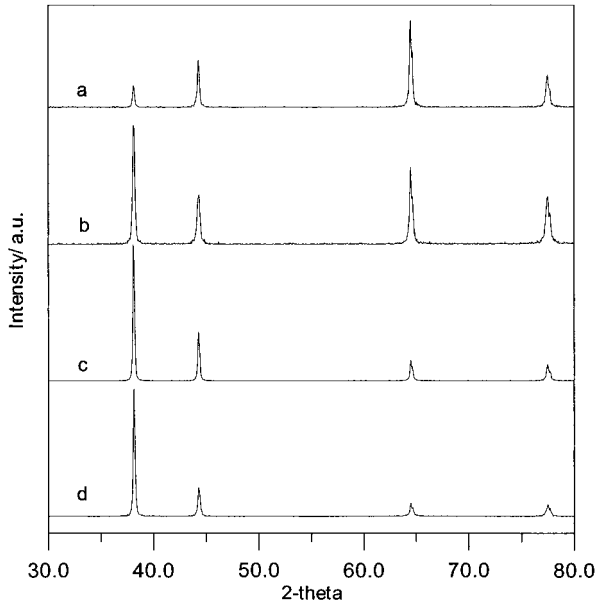

Figure 2. XRD patterns of different gold substrates with different predominant crystalline orientations before ORC treatments.

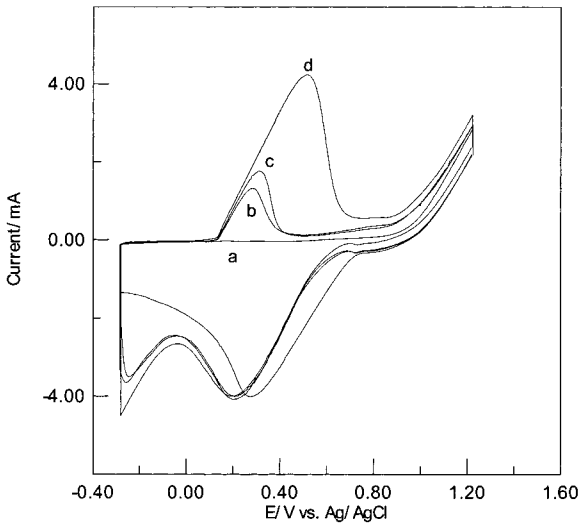

Figure 3. Cyclovoltammograms of the 25th scan of the redox processes occurring on Au substrates with different crystalline orientations, as shown in Figure 2, in 0.1 M KCl at 500 mV/s.

The mechanism of the roughening procedure on gold and the corresponding Au-based complex formed will be further discussed later.

To investigate the differences of crystalline orientations of gold before ORC treatment and redeposition gold after ORC treatment, the redeposited gold powders were carefully scraped down from the gold substrate and were collected eight times. Then XRD analyses were performed on the scraped powders. Figure 4 shows the results. The ratio of the intensity of the (111) face to the intensity of the (220) face of sample (a) with a predominant (220) face increases from 0.245 to 0.461. Similarly but less significantly, the ratio of the intensity of the (111) face to the intensity of the (220) face of sample (c) with a predominant (111) face increases from 6.54 to 8.92. A study of SERS of a Cu/Pd alloy colloid by Lu et al.[9] indicates that the Cu-rich particles spanning from 2 to 10 nm in size display an increase in the (111) lattice spacings compared to the bulk state. Chen et al.[29] reported an in situ electrochemical scanning tunneling microscopy study of the structural changes of silver surfaces following an ORC. The result indicates that the low index plane (111) has the lowest surface energy. The growth of this crystal plane becomes apparent after an ORC. Since gold, silver, and copper have the same forms of crystal lattices, an increase in the intensity of (111) orientation of gold after ORC treatment shown in Figure 4 is a reasonable phenomenon.

Characteristics of PPy Films Deposited on Roughened Au. As reported in the previous study,[30] no meaningful information can be provided from the Raman spectroscopy of PPy deposited on an Au substrate without ORC treatment. However, almost all of the scattering modes of PPy can be markedly demonstrated with sharp peaks, due to the SERS effect. Figure 5 shows the Raman spectra of PPy deposited on roughened gold substrates with different predominant orientations of (111) and (220), respectively. Obviously, a PPy spectrum obtained on roughened gold with a predominant (111) orientation exhibits both higher intensity, more than four times, and more excellent resolution. This increase in intensity is significant in comparison with the report of polyaniline chemically deposited on various rough metals by Baibarac et al.[27] These phenomena of higher intensity and resolution of PPy spectrum obtained on roughened Au with predominant (111) orientation can be explicated from the following XRD analyses. Figure 6 shows the XRD patterns of PPy films deposited on different gold substrates. As reported

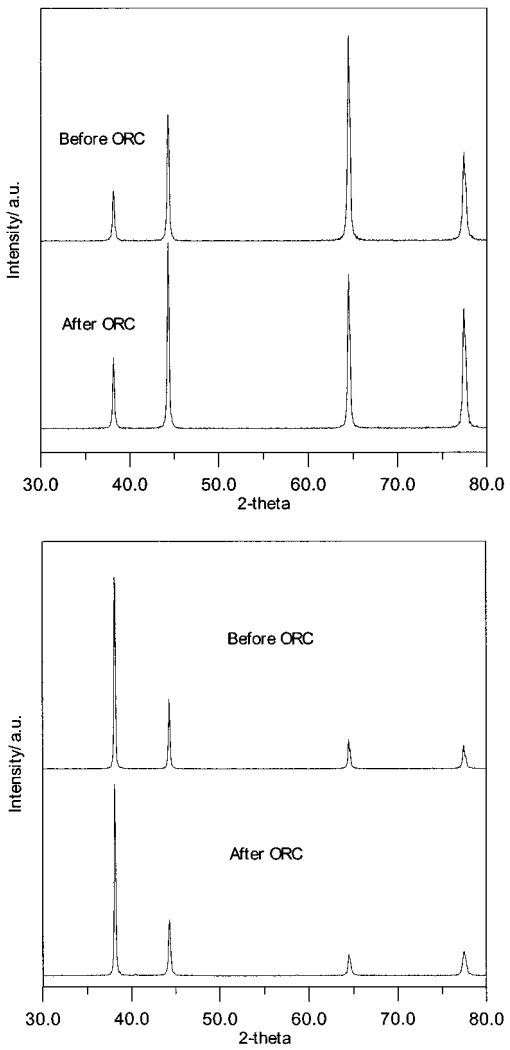

Figure 4. XRD patterns of different gold substrates with different predominant crystalline orientations before and after ORC treatments. (a) Sample (a) with predominant (220) orientation, as shown in Figure 2. (b) Sample (c) with predominant (111) orientation, as shown in Figure 2.

in the previous study,[31] the PPy film deposited on mechanically polished Pt is amorphous. This amorphous structure is similarly observed on pattern (c) in Figure 6. However, as revealed from patterns (a) and (b), the surface texture of PPy seems to be of ordered arrangement toward the orientations of gold substrates, especially for PPy deposited on roughened Au with the predominant (111) orientation. In the study of XRD pattern of Cu deposited on Cu and PPy substrates by Chen et al.,[32] they also found that the surface structure is strongly affected by the microstructure of the substrate surface. Parsons[22] reported that the strongest adsorption of chloride on silver occurs on the (111) surface with the lowest surface energy. Meanwhile, highly ordered monolayer films were found to be self-assembled onto Au (111) in the study by Caldwell et al.[26] In this study, SERS spectra are measured on the roughened gold substrates. PPy films incline to be deposited on the (111) face with the lowest surface energy, and these films demonstrate a marked order in character. These would be contributive to higher intensity and resolution of Raman spectra obtained. Also, these results are consistent with the reports that SERS is sensitive to molecular orientation and to direct proximity with the substrate, as shown in the literature.[24,25]

Mechanism of Roughening Procedure in CV. Figure 7 shows the redox process occurring on the gold with scan. The

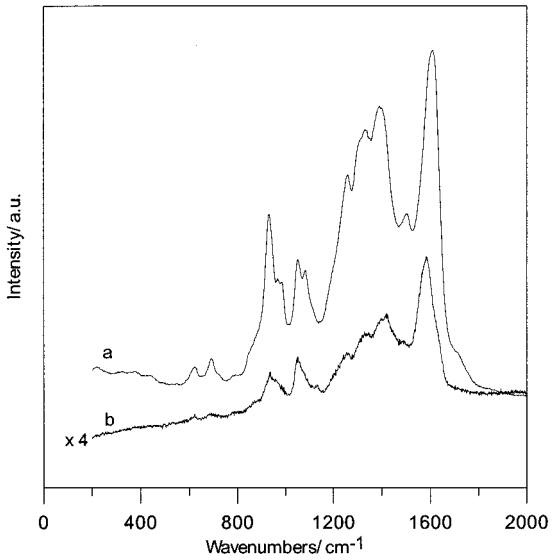

Figure 5. Raman spectra of 10 mC PPy films deposited on roughened Au substrates with different predominant orientations. (a) With (111) predominant orientation. (b) With (220) predominant orientation; the intensity was magnified by 4-fold.

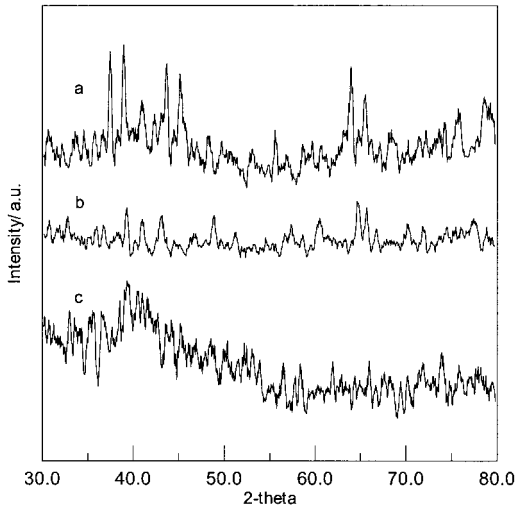

Figure 6. XRD patterns of 500 mC PPy films deposited on different gold substrates. (a) Gold with predominant (111) orientation roughened by ORC treatment. (b) Gold with predominant (220) orientation roughened by ORC treatment. (c) Mechanically polished gold with predominant (111) orientation without ORC treatment.

anodic peak located at ca. 0.2 V vs Ag/AgCl initially shows at the 8th scan. Then this anodic peak becomes larger and the peak potential anodically increases with an increase of scan numbers. The onset of gold dissolution occurring at around 0.9 V vs Ag/AgCl forms predominantly $AuCl_4^-$.[33] The oxygen evolution occurs significantly in competition with gold dissolution at potential more positive than 1.0 V vs Ag/AgCl. At potential more negative than −0.1 V vs Ag/AgCl, the hydrogen evolution also occurs. Correspondingly, the desorption of hydrogen occurs at ca. 0.3 V vs Ag/AgCl with the anodic scan. At this anodic peak, hydrogen desorption would be accompanied with the formation of $Au(ClO_4)_4^-$, which will be further confirmed, because the hydrogen evolution does not increase with the increase of the anodic peak at scan over 15 ones in ORC. Also, this redox reaction of hydrogen evolution and desorption does not show on gold with predominant (220) orientation, as illustrated in Figure 3. To ascertain the reactions at anodic and cathodic vertexes, different CV experiment used various vertexes

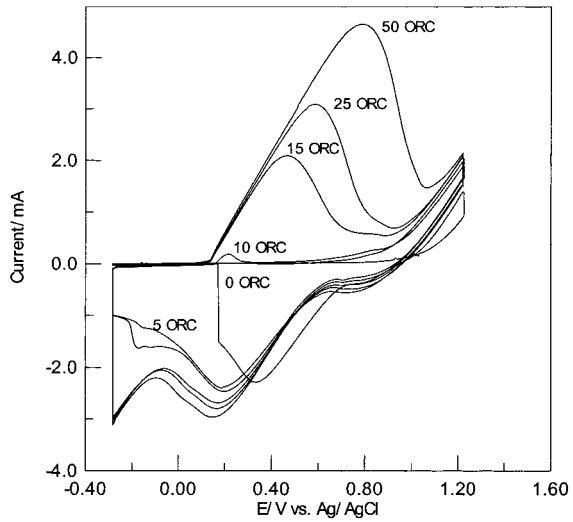

Figure 7. Cyclovoltammograms of different scans of the redox processes occurring on Au substrate with predominant (111) crystalline orientation in 0.1 M KCl at 500 mV/s.

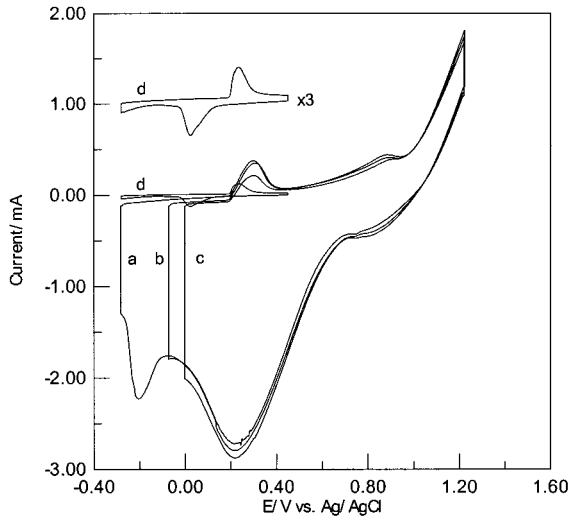

Figure 8. Cyclovoltammograms of the redox processes occurring on Au substrate with predominant (111) orientation in 0.1 M KCl at 500 mV/s with different vertexes potentials. (a) −0.28 to 1.22 V vs Ag/AgCl. (b) −0.07 to 1.22 V vs Ag/AgCl. (c) −0.0 to 1.22 V vs Ag/AgCl. (d) −0.28 to 0.45 V vs Ag/AgCl.

potentials were performed, as shown in Figure 8. In case of changing the cathodic vertex toward the positive potential from −0.28 to 0 V vs Ag/AgCl, the hydrogen evolution reduces. Correspondingly, the anodic peak at ca. 0.3 V vs Ag/AgCl partially representing the hydrogen desorption diminishes. In case of changing the anodic vertex toward the negative potential from 1.22 to 0.45 V vs Ag/AgCl, the broader cathodic peak at ca. 0.2 V vs Ag/AgCl associated with the reductions of compounds formed at the anodic potential of 1.22 V vs Ag/AgCl disappears, with a possible redox reaction of Au and Au^+ instead.[19]

The Cl and Au-containing complex formed on the roughened Au can be confirmed via XPS analyses. Figure 9 shows the XPS Cl 2p core-level spectra of roughened Au substrates with different crystalline orientations. The main peaks of the chloride-contained complexes formed on Au substrates with different predominant orientations of (111) and (220) are located at 208 and 199 eV, respectively. These chloride peaks at 208 and 199 eV are assigned to Cl (+7) and Cl (−1), respectively.[34] Figure 10 displays the $Au4f_{7/2-5/2}$ doublet region of roughened Au with

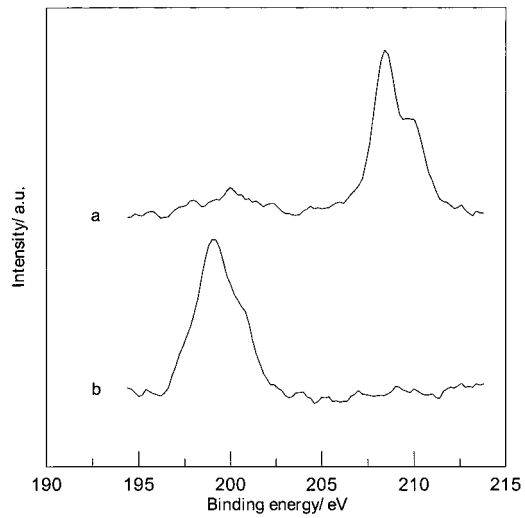

Figure 9. XPS Cl 2p core-level spectra of gold substrates with different crystalline orientations roughened by ORC treatment of 25 scans. (a) With predominant (111) orientation. (b) With predominant (220) orientation.

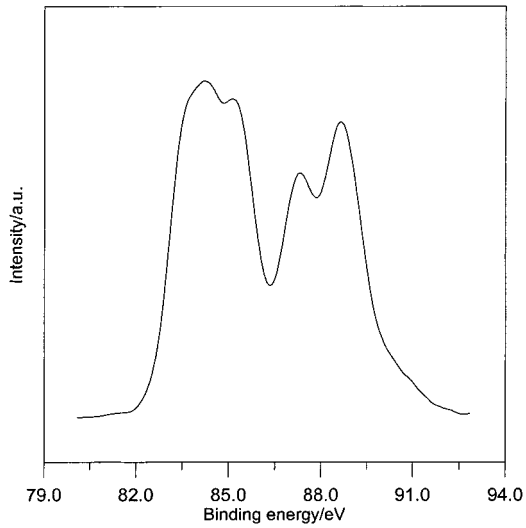

Figure 10. XPS Au4f$_{7/2-5/2}$ core-level spectrum of the gold substrate with predominant (111) orientation roughened by ORC treatment of 25 scans.

predominant (111) orientation. In this figure, redeposited Au powders with different oxidation states, scraped down and collected from the roughened Au for 10 times, were found after the Au substrate was roughened by ORC treatment. The oxidized Au can be assigned to monovalent Au(I) and trivalent Au(III) at 85.2 and 86.7 eV, respectively.[35] No further deconvolution was made and trivalent Au(III), as usually shown in the Cl and Au-containing complex,[21,33,36] was adopted in this study. Combining the electronic configuration of Cl shown in Figure 9, the complexes can be assigned to $Au(ClO_4)_4^-$ and $AuCl_4^-$ formed on the Au substrates with predominant orientations of (111) and (220), respectively.

From the discussion above, the roughing procedure and chloride-contained complex formed in ORC, being closely related with the SERS effect, can be exactly concluded. In case of gold with predominant (220) orientation, $AuCl_4^-$ is predominantly formed on the electrode, as shown in the literature.[13,21,33] In the case of gold with predominant (111) orientation, Cl^- is easily adsorbed on this (111) face.[22] The roughing procedure can be summarized as follows.

In anodic scan:

$$Au \rightarrow Au^{3+} + 3e^- \quad \text{(dissolution)} \quad (1)$$

$$Au^{3+} + 4Cl^- \rightarrow AuCl_4^- \quad \text{(primary complex formation on (111) face)} \quad (2)$$

At the anodic vertex:

$$2H_2O \rightarrow O_2 + 4e^- \quad \text{(oxygen evolution)} \quad (3)$$

In cathodic scan:

$$O_2 + 4e^- \rightarrow 2O^{2-} \quad \text{(oxygen reduction)} \quad (4)$$

At anodic peak of ca. 0.3 V vs Ag/AgCl:

$$AuCl_4^- + 16O^{2-} \rightarrow Au(ClO_4)_4^- + 32e^- \quad \text{(final complex formation)} \quad (5)$$

Conclusion

In this study, PPy films were electrochemically deposited on roughened gold substrates with different predominant crystalline orientations of (111) and (220), respectively. The result indicates that the (220) crystalline orientation of gold was partially changed into (111) orientation after gold was roughened with ORC treatment. The SERS spectroscopy of PPy deposited on gold with a predominant (111) orientation exhibits higher intensity, more than 4-fold, and more excellent resolution. Meanwhile, the redox behavior and complex formed on gold in ORC was strongly sensitive to the crystalline orientation. The complexes are $Au(ClO_4)_4^-$ and $AuCl_4^-$ for Au substrates with predominant orientations of (111) and (220), respectively. A mechanism of the roughening procedure on gold was strictly proposed to illustrate the resulting complex and its effect on the SERS enhancement.

Acknowledgment. The authors thank the National Science Council of the Republic of China (NSC-90-2214-E-238-001) and Van Nung Institute of Technology for their financial support.

References and Notes

(1) Schantz, S.; Torell, M. *J. Appl. Phys.* **1988**, *64*, 2038.
(2) Kim, D. Y.; Lee, J. Y.; Moon, D. K.; Kim, C. Y. *Synth. Met.* **1995**, *69*, 471.
(3) Oddi, L.; Capelletti, R.; Fieschi, R.; Fontana, M. P.; Ruani, G. *Mol. Cryst. Liq. Cryst.* **1985**, *118*, 179.
(4) Inoue, T.; Hosoya, I.; Yamase, T. *Chem. Lett.* **1987**, 563.
(5) Grasselli, J. G.; Bulkin, B. J. *Analytical Raman Spectroscopy*; John Wiley & Sons: New York, 1991; pp 295−298.
(6) Plays, B. J.; Bukowska, J.; Jackowska, K. *J. Electroanal. Chem.* **1997**, *428*, 19.
(7) Roy, D.; Furtak, T. E. *Chem. Phys. Lett.* **1986**, *124*, 299.
(8) Lefrant, S.; Baltog, I.; Baibarav, M.; Journet, G. C.; Bernier, P. *Synth. Met.* **1999**, *101*, 184.
(9) Lu, P.; Dong, J.; Toshima, N. *Langmuir* **1999**, *15*, 7980.
(10) Van Duyne, R. P.; Hulteen, J. C.; Triechel, D. A. *J. Chem. Phys.* **1993**, *99*, 2101.
(11) Bukowska, J.; Jackowska, K. *Electrochim. Acta* **1990**, *35*, 315.
(12) Pemberton, J. E.; Guy, A. L.; Sobocinski, R. L.; Tuschel, D. D.; Cross, N. A. *Appl. Surf. Sci.* **1988**, *32*, 33.
(13) Gao, P. M.; Patterson, L.; Tadayyoni, M. A.; Weaver, M. J. *Langmuir* **1985**, *1*, 173.
(14) Taylor, C. E.; Pemberton, J. E.; Goodman, G. G.; Schoenfisch, M. H. *Appl. Spectrosc.* **1999**, *53*, 1212.
(15) Devine, T. M.; Furtak, T. E.; Macomber, S. H. *J. Electroanal. Chem.* **1984**, *164*, 299.
(16) Cai, W. B.; Ren, B.; Li, X. Q.; She, C. X.; Liu, F. M.; Cai, X. W.; Tian, Z. Q. *Surf. Sci.* **1998**, *406*, 9.

(17) Takahashi, M.; Niwa, M.; Ito, M. *J. Phys. Chem.* **1987**, *91*, 11.
(18) Bandyopadhyay, K.; Vijayamohanan, K. *Langmuir* **1999**, *15*, 5314.
(19) Hesse, E.; Creighton, J. A. *Langmuir* **1999**, *15*, 3545.
(20) Gao, P.; Weaver, M. J. *J. Phys. Chem*. **1985**, *89*, 5040.
(21) Gao, P.; Gosztola, D.; Leung, L. W. H.; Weaver, M. J. *J. Electroanal. Chem.* **1987**, *233*, 211.
(22) Parsons, R. *J. Electroanal. Chem.* **1981**, *118*, 3.
(23) Bukowska, J.; Jackowska, K.; Jaszczynski, K. *J. Electroanal. Chem.* **1989**, *260*, 373.
(24) Furtak, T. E.; Roy, D. *Surf. Sci.* **1985**, *158*, 126.
(25) Demuth, J. E.; Christmann, K.; Sanda, P. N. *Chem. Phys. Lett.* **1980**, *76*, 201.
(26) Caldwell, W. B.; Campbell, D. J.; Chen, K.; Herr, B. R.; Mirkin, C. A.; Malik, A.; Durbin, M. K.; Dutta, P.; Huang, K. G. *J. Am. Chem. Soc.* **1995**, *117*, 6071.
(27) Baibarac, M.; Cochet, M.; Lapkowski, M.; Mihut, L.; Lefrant, S.; Baltog, I. *Synth. Met.* **1998**, *96*, 63.
(28) Chang, R. K.; Laube, B. L. *CRC Crit. Rev. Solid State Mater. Sci.* **1984**, *12*, 1.
(29) Chen, J. S.; Devine, T. M.; Ogletree, D. F.; Salmeron, M. *Surf. Sci.* **1991**, *258*, 346.
(30) Liu, Y. C.; Hwang, B. J.; Jian, W. J.; Santhanam, R. *Thin Solid Film* **2000**, *374*, 85.
(31) Liu, Y. C.; Hwang, B. J. *Thin Solid Films* **1999**, *339*, 233.
(32) Chen, S. K.; Wang, Y. Y.; Wan, C. C. *Mater. Sci. Eng., B* **1994**, *27*, 103.
(33) Gaur, J. N.; Schmid, G. M. *J. Electroanal. Chem.* **1970**, *24*, 279.
(34) Schmeisser, D.; Naaemann, H.; Gopel, W. *Synth. Met.* **1993**, *59*, 211.
(35) Suzer, S.; Ertas, N.; Kumser, S.; Ataman, O. Y. *Appl. Spectrosc.* **1997**, *51*, 1537.
(36) Henry, M. C.; Hsueh, C. C.; Timko, B. P.; Freund, M. S. *J. Electrochem. Soc.* **2001**, *148*, D155.